Tetrahedron 64 (2008) 10049–10054

Contents lists available at ScienceDirect

Tetrahedron

journal homepage: www.elsevier.com/locate/tet

Synthesis of de novo designed small-molecule inhibitors of bacterial RNA polymerase

Anil K. Agarwal, A. Peter Johnson *, Colin W.G. Fishwick *

School of Chemistry, University of Leeds, Leeds LS2 9JT, UK

ARTICLE INFO

Article history:
Received 28 May 2008
Received in revised form 27 July 2008
Accepted 14 August 2008
Available online 16 August 2008

ABSTRACT

The de novo molecular design program SPROUT has been used in conjunction with the X-ray crystal structure of RNA polymerase (RNAP) from *Thermus aquaticus* to produce a novel enzyme inhibitor scaffold. A short and efficient synthesis of molecules corresponding to this scaffold has been developed and in keeping with the design predictions, the resulting inhibitors displayed useful levels of inhibition of *Escherichia coli* RNAP.

1. Introduction

The global emergence of bacterial resistance to existing antibiotics is a serious public health issue. Indeed, the World Health Organization estimates that infection by antibiotic resistant bacteria more than doubles the risk of death.[1,2] Consequently, there remains an urgent need to discover and develop new antibiotics to counteract resistance. Traditionally, the pharmaceutical industry has adopted analogue improvement programmes to develop new antibiotics whereby derivatives of established classes (e.g., β-lactams, quinolones, macrolides, tetracyclines, sulfonamides) with improved activity against existing resistant isolates have been introduced.[3] However, opportunities for further chemical modification of existing classes are now diminishing and a consensus is also emerging that new antibiotics should not simply be analogues of existing classes since pre-existing bacterial mechanisms of resistance rapidly evolve to confer resistance to new derivatives.[4]

Bacterial RNA polymerase (RNAP) is an attractive drug target.[5,6] It plays an essential role in transcription in all bacteria and consequently drugs that inhibit this enzyme are likely to have a broad spectrum of activity affecting both Gram-positive and Gram-negative pathogens.[6] Bacterial core RNAP is a stable, noncovalent assembly of four essential polypeptide chains with the subunit composition β, β, 2α.

The roles of the individual subunits have been defined and functional sites, or regions of importance for subunit interactions, have been identified.[7] Promoter-specific initiation of transcription requires both core RNAP and a sigma factor, which together comprise the holoenzyme. Thus, RNAP contains a number of functionally distinct and essential sites, which may be amenable to inhibition by antibacterial drugs. Bacterial RNAP is structurally distinct from mammalian RNAPs[7] permitting selective design of bacterial inhibitors. Antisense knock-down technology demonstrates that RNAP is essential for bacterial growth and survival and the potent bactericidal antibiotic rifampicin, which specifically targets bacterial RNAP, has been in medical use for over 40 years to treat infectious diseases.[8,9] Rifampicin binds close to the active site of the catalytic β subunit and inhibits initiation of RNA synthesis. Indeed, rifampicin, which is a bactericidal antibiotic, is an important component of anti-TB therapies and is also used to treat staphylococcal infections.[10] These observations provide proof of principle that inhibition of RNAP can lead to successful chemotherapeutic intervention of infections, including those caused by *Mycobacterium tuberculosis* and *Staphylococcus aureus*. Although there is still interest in developing members of the rifamycin class for the chemotherapy of bacterial infections[11–15] the progressive emergence of RNAP mutants resistant to rifamycins makes it more appealing to search for novel RNAP inhibitors not subject to cross-resistance with existing rifamycin antibiotics. However, a recent report, from a major pharmaceutical company, summarising their work in antibacterial drug discovery has indicated that RNAP is a challenging target in terms of hit identification using traditional high throughput screening of large compound libraries.[16]

As part of a structure-based design and synthesis program for the discovery of new enzyme inhibitors, we have previously described the computer-aided molecular design, synthesis and biological evaluation of novel inhibitors targeted at the bacterial D-ala-D-ala ligase,[17] the bacterial D-glu adding ligase MurD[18] and the *Plasmodium* dihydroorotate dehydrogenase[19,20] enzymes, respectively. Here, we describe the first non-macrocyclic bacterial RNAP inhibitors, designed to target the rifampicin binding site, which were created using a fragment-based de novo design approach.

* Corresponding authors. Tel.: +44 (0) 113 343 6510; fax: +44 (0) 113 343 6565.
E-mail addresses: p.johnson@leeds.ac.uk (A.P. Johnson), colinf@chem.leeds.ac.uk (C.W.G. Fishwick).

0040-4020/$ – see front matter © 2008 Elsevier Ltd. All rights reserved.
doi:10.1016/j.tet.2008.08.037

The structure-based design of small-molecule enzyme inhibitors is a powerful tool in drug discovery, particularly when there is an X-ray crystal structure of the target enzyme available. In particular, fragment-based de novo methods offer a rapid and powerful approach to inhibitor design, which can complement other in silico approaches such as virtual high throughput screening.[21–24]

The X-ray crystal structure of the complex formed between core RNAP from *Thermus aquaticus* and rifampicin has been reported to 3.3 Å resolution.[7] This structure reveals that rifampicin binds to the enzyme within a cleft located approximately 12.1 Å away from the active site in a region in which the newly synthesised RNA polymer leaves the complex. Rifampicin inhibits RNAP by preventing formation of RNA beyond the addition of two to three nucleotides. Additionally, since rifampicin binds remotely from the active site and in a region of bacterial RNAP that is structurally different from that in the human RNAP II, the antibiotic has low toxicity.

The binding site of rifampicin is revealed to be a fairly open cavity, which is substantially exposed to solvent. Rifampicin makes several specific hydrogen bond contacts to residues within the RNAP including S411, R409, H406, F394 and Q390 (Fig. 1, *Escherichia coli* numbering used throughout). Additionally, several residues have important roles in contributing to hydrophobic interactions with rifampicin including R405, H52, L391, L413, Q390, S392, D396 and F394.

In terms of the design of new inhibitors, the rifampicin binding site poses a number of challenges, mainly due to the rather solvent-exposed nature of the binding site, its relatively large surface area, and the general lack of compact binding pockets within which to locate small-molecule inhibitors. We reasoned, therefore, that a fragment-based modular design approach, such as that used within the SPROUT[25–27] molecular design software, would offer good prospects for the production of novel RNAP inhibitors targeting this binding cavity.

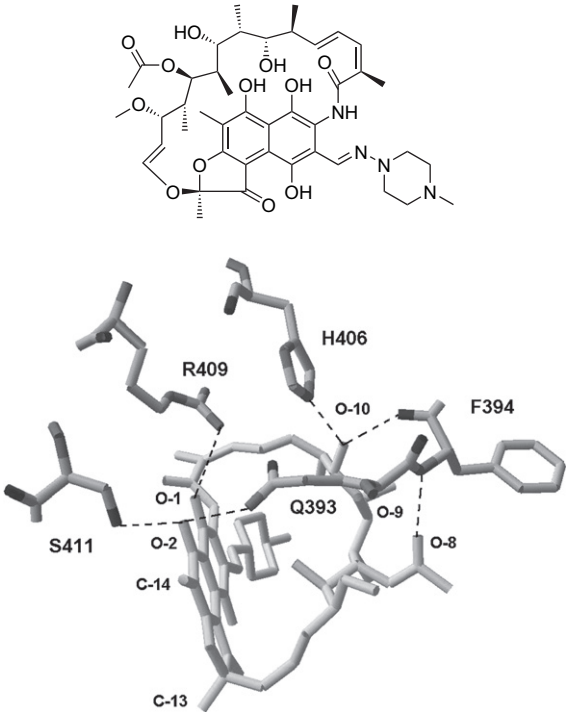

Figure 1. (Top) Structure of rifampicin; (bottom) important H-bond contacts of rifampicin to RNAP.

2. Results and discussion

Analysis, using SPROUT, of the inhibitor binding potential within this cavity revealed the presence of additional binding sites not utilised by rifampicin (Fig. 2). It was reasoned that a cluster of five specific hydrogen-bonding sites (involving residues Q390, F394, R405, Q567 and Q633), in addition to a region of relatively high hydrophobicity (located near to Q390 and R405), offered good prospects for the design of small-molecule inhibitors.

The fragment-based molecular design approach utilised within SPROUT typically involves the docking of small molecular fragments into each of the chosen binding sites followed by joining of these docked fragments to yield sets of designed inhibitor templates. These are then ranked using a number of criteria including predicted binding affinity, molecular complexity and synthetic accessibility, to reveal the best inhibitor candidates for laboratory synthesis and biological evaluation. Application of this fragment-based inhibitor design approach to the six chosen binding sites within the rifampicin binding cavity of RNAP yielded a simple, synthetically attractive molecular template **1** based on a 1,2,4,6-tetrasubstituted aromatic core (Fig. 2).

In addition to the highly substituted aromatic core, the design template required the hydrogen bond donor (shown as an N–H in structure **1** in Scheme 1 below), which makes contact with the backbone carbonyl group of F394 and, which is connected to a stereocentre with '*R*' absolute stereochemistry. In addition to two substituents designed to accept hydrogen bonds from the side-chains of residues R405 and Q567, respectively, the designed template **1** includes a second aromatic ring designed to reside

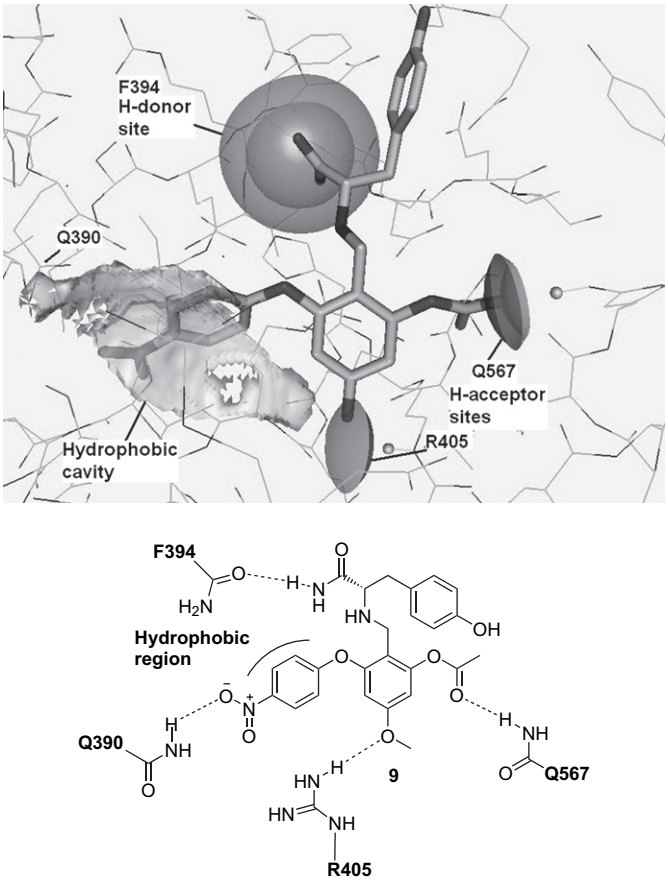

Figure 2. (Top) SPROUT-analysis of designed inhibitor template **1** bound within RNAP. The hydrophobic region and the H-bonding sites utilised in the design are shown as shaded regions; (bottom) schematic showing bonding interactions of SPROUT-designed inhibitor 9.

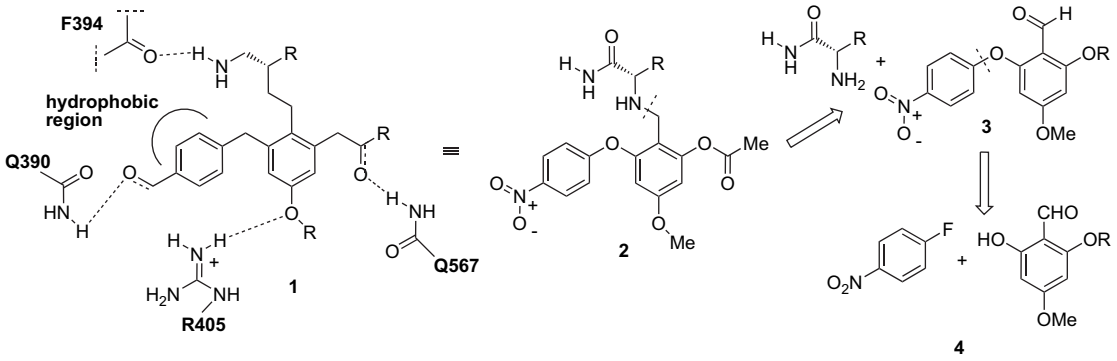

Scheme 1. (Left) SPROUT-generated RNAP inhibitor template **1** and synthetic equivalent **2**; (right) synthetic approach to inhibitors **2**.

within the hydrophobic region flanked by residues Q390 and R405. This ring also incorporates a *para*-substituent designed to make a hydrogen bond to the side chain of Q390 (Scheme 1).

Structural analysis of the designed template **1** with respect to synthetic accessibility led to the identification of amino acid-derived systems **2** (Scheme 1). It was envisaged that these systems would be easily prepared, in optically active form, via reductive amination of a suitably functionalised 2,4,6-trisubstituted benzaldehyde **3** (available via O-arylation of phenols **4** with 4-fluoronitrobenzene) with readily available amino acid amides (Scheme 1).

Two representative examples of inhibitors **1** were readily prepared using this synthetic approach (Scheme 2).

As shown below (Scheme 2), the first step involves an *ipso* substitution reaction between 4-fluoronitrobenzene and 3, 5-dimethoxyphenol to yield ether **5**, which, on Vilsmeier formylation, yielded aldehyde **6**.

The selective demethylation of **6** worked well using the literature method[28] giving phenol **7** in good yield, which was then acetylated to yield the key aldehyde **8** (Scheme 2). Reductive amination of aldehyde **8**, using commercially available amino acid amides, yielded the target molecules (**9** and **10**).

Inhibitors **9** and **10** were screened for their ability to inhibit *E. coli* RNAP using the SYBR Green assay.[29] Preliminary experiments revealed that compounds **9** and **10** inhibited RNAP activity with IC_{50} values of 70 μM and 62 μM, respectively. In addition to enable the facile synthesis of inhibitors **9** and **10**, the nitro group present in these systems was included so as to contact Q390. Although, it was reasoned that this would involve donation of an H-bond from the side chain NH_2 of Q390, at the resolution of the crystal structure, we reasoned that it was possible for the carbonyl oxygen and the NH_2 moieties of this side chain to be reversed. This would require an H-bond donor within the inhibitors at the position currently occupied by the nitro group position. In order to explore this alternative H-bonding possibility, the nitro groups in inhibitors **9** and **10** were selectively reduced in the presence of the benzyl amine moiety to the corresponding amines **11** and **12** using PtO_2 as the catalyst (Scheme 3).

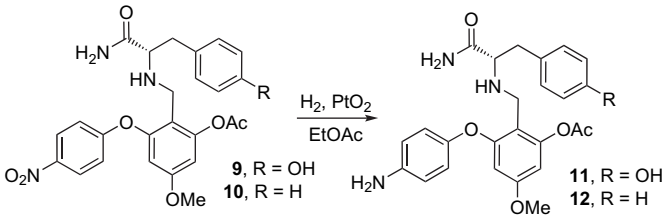

Scheme 3. Preparation of amino-derivatives.

Inhibitor **11** was threefold less active than the corresponding nitro version **9** and inhibitor **12** was found to be inactive in the SYBR Green assay. These results suggest that the H-bonding between Q390 and the designed inhibitors are as shown in Figure 2. It is interesting to note, however, that Diederich et al. have suggested that nitro groups are relatively poor H-bond acceptors.[30,31]

3. Conclusions

In summary, a fragment-based molecular design approach together with a very short and efficient synthesis has been used, for the first time, to produce a novel type of inhibitor, designed to target the rifampicin binding cavity of bacterial RNAP. Although preliminary experiments indicate that these molecules inhibit the operation of bacterial RNAP, clearly more work is needed in order to

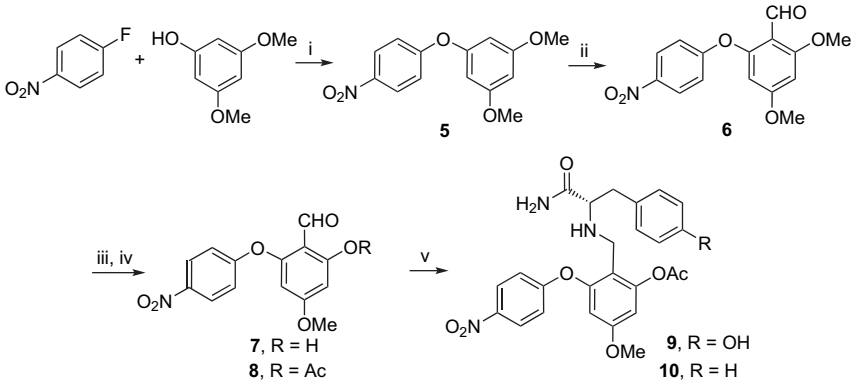

Scheme 2. Reagents and conditions: (i) K_2CO_3, DMF, 40 °C, 93%; (ii) DMF, $POCl_3$, 80 °C, 58%; (iii) BCl_3, DCM, 70 °C, 95%; (iv) AcCl, Et_3N, DCM, 0 °C, 80%; (v) L-tyrosinamide or L-phenylalaninamide, AcOH, DCM/THF (1:1), $NaBH(OAc)_3$, 53%.

probe the details of this inhibitory activity. Additionally, although we appreciate that this type of inhibitor is not really 'drug-like', the power of this approach in the rapid identification of bacterial RNAP inhibitors is underlined by the recently reported failure of classical HTS methods to identify RNAP inhibitors.[16] We believe that our approach to ligand design, where specific small-molecule fragments are matched to particular features within the protein, is particularly advantageous when applied to rather open and solvent-exposed binding cavities such as the rifampicin binding region of bacterial RNAP. Additionally, via careful selection of the contacting sites within the protein to be used by the designed inhibitor, it should be possible to design such inhibitors that do not rely on making contacts to residues prone to resistance mutations and may yield inhibitors active against bacteria resistant to existing antibiotics such as rifampicin. We are currently extending these findings to develop more drug-like inhibitors possessing such novel antibacterial activity and will report these results elsewhere.

4. Experimental

4.1. General

Infrared spectra were recorded using a Nicolet Avatar 300 FT-IR spectrophotometer. The vibrational frequencies are reported in wave numbers (cm^{-1}). ^1H and ^{13}C NMR spectra were measured on Bruker DPX300 Fourier transform spectrometer using an internal deuterium lock using tetramethylsilane as the internal standard. Coupling constants (J) are quoted in hertz (Hz). Low and high resolution mass spectra were recorded on a VG Autospec mass spectrometer, operating at 70 eV, using either chemical ionisation (CI), electron impact (EI) or fast atom bombardment (FAB) ionisation techniques. All accurate mass measurements were performed using a ZMD mass spectrometer using ES. Optical rotations were determined using an Optical Activity AA1000 polarimeter with cells of path lengths 0.25 or 1 dm. Melting points were determined using a Reichert hot stage and are uncorrected. Microanalyses were performed by the University of Leeds Microanalytical service using an Elemental Analyser 1106. Flash column chromatography was carried out using Merck Kieselgel 60 (230–400 mesh). Solvents were either obtained dry from commercial sources or dried prior to use using standard methods.

4.1.1. 1,3-Dimethoxy-5-(4-nitrophenoxy) benzene (**5**)

K_2CO_3 (4.0 g, 28.4 mmol) was added to a solution of 3,5-dimethoxyphenol (2.2 g, 14.2 mmol) in DMF (20 ml) and stirred for 15 min. A solution of 1-fluoro-4-nitrobenzene (2.0 g, 14.2 mmol) in DMF (10 ml) was added and the reaction mixture was then stirred at 40 °C for 6 h. The reaction mixture was cooled, poured into crushed ice (50 g) and stirred for 30 min. The precipitate was filtered, washed with water (20 ml) and dried in vacuo to yield the title compound **5** (3.5 g, 12.7 mmol, 90% yield) as colourless plates, which needed no further purification. Mp 117–118 °C. R_f 0.66 (petrol/EtOAc, 8:2). ^1H NMR (300 MHz, $CDCl_3$): δ 8.20 (dd, 2H, J_{HH} 7.0, 2.0, Ar–H), 7.04 (dd, 2H, J_{HH} 7.1, 2.1, Ar–H), 6.35 (t, 1H, J_{HH} 2.2, Ar–H), 6.23 (d, 2H, J_{HH} 2.2, Ar–H), 3.78 (s, 6H, OMe). ^{13}C NMR (75 MHz, $CDCl_3$): 163.46, 162.34, 156.81, 143.11, 126.69, 117.72, 99.33, 97.83, 55.97 (OMe). ν_{max}/cm^{-1}: 2843, 1601, 1459, 1342, 1208, 1154, 1116, 1048; m/z (ES): 276 (M^++1); Found: C, 60.8; H, 4.95; N, 5.3%. $C_{14}H_{13}NO_5$ requires: C, 61.09; H, 4.76; N, 5.09%.

4.1.2. 2,4-Dimethoxy-6-(4-nitrophenoxy) benzaldehyde (**6**)

Phosphoryl chloride (5.0 ml, 55.0 mmol) was carefully added to ice-cold DMF (4.2 ml, 55.0 mmol) at 0 °C. A solution of 1, 3-dimethoxy-5-(4-nitrophenoxy) benzene **5** (3.0 g, 11.0 mmol) in DMF (10 ml) was added and the resulting mixture was heated at 80 °C for 3 h. The dark viscous mixture was then poured into ice-cold water (50 ml) and stirred vigorously for 2 h to coagulate any precipitate, which was filtered off. The precipitate was washed with water (50 ml), dried and chromatographed [DCM/EtOAc, 99:1] to yield the title compound **6** (1.9 g, 6.3 mmol, 58% yield) as colourless plates. Mp 115–116 °C. R_f 0.83 (DCM/EtOAc, 95:5). ^1H NMR (300 MHz, $CDCl_3$): δ 10.25 (s, 1H, Ar–CHO), 8.20 (dd, 2H, J_{HH} 7.0, 2.1, Ar–H), 7.00 (dd, 2H, J_{HH} 7.0, 2.1, Ar–H), 6.39 (d, 1H, J_{HH} 2.1, Ar–H), 6.18 (d, 1H, J_{HH} 2.1, Ar–H), 3.95 (s, 3H, OMe), 3.85 (s, 3H, OMe). ^{13}C NMR (75 MHz, $CDCl_3$): 186.77 (Ar–CHO), 166.51, 164.79, 163.33, 157.93, 143.26, 126.38, 117.21, 112.12, 99.85, 96.14, 56.69 (OMe), 56.32 (OMe). ν_{max}/cm^{-1}: 2985, 2883, 2794, 1690 (CO), 1608, 1486, 1414, 1335, 1242, 1147; m/z (ES): 304 (M^++1); Found: C, 59.3; H, 4.4; N, 4.45%. $C_{15}H_{13}NO_6$ requires: C, 59.41; H, 4.32; N, 4.62%.

4.1.3. 2-Hydroxy-4-methoxy-6-(4-nitrophenoxy) benzaldehyde (**7**)

Boron trichloride (8.5 ml, 1 M solution in DCM, 8.5 mmol) was added during 20 min to a stirred solution of 2,4-dimethoxy-6-(4-nitrophenoxy) benzaldehyde **6** (1.6 g, 5.3 mmol) in DCM (20 ml) cooled to −70 °C. The resulting pale yellow solution was allowed to warm to rt, stirred at this temperature for 3 h, and then poured with stirring into ice-cold 1 M HCl (50 ml). The DCM layer was separated, washed with water (3×30 ml) and brine (30 ml), dried ($MgSO_4$) and evaporated to dryness. The crude solid was chromatographed to yield the title compound **7** (1.45 g, 5.0 mmol, 95% yield) as colourless needles. Mp 150–151 °C. R_f 0.4 (petrol/EtOAc, 8:2). ^1H NMR (300 MHz, $CDCl_3$): δ 10.07 (s, 1H, Ar–CHO), 8.28 (dd, 2H, J_{HH} 7.0, 2.1, Ar–H), 7.18 (dd, 2H, J_{HH} 7.0, 2.1, Ar–H), 6.27 (d, 1H, J_{HH} 2.2, Ar–H), 5.94 (d, 1H, J_{HH} 2.2, Ar–H), 3.82 (s, 3H, OMe). ^{13}C NMR (75 MHz, $CDCl_3$): 191.66 (Ar–CHO), 168.10, 166.67, 161.76, 159.89, 144.36, 126.60, 119.33, 107.98, 98.81, 97.45, 56.45 (OMe). ν_{max}/cm^{-1}: 3080, 2928, 2447, 1921, 1782 (CO), 1748, 1509, 1336, 1156, 1107; m/z (ES): 290 (M^++1); Found: C, 58.4; H, 4.1; N, 4.75%. $C_{14}H_{11}NO_6$ requires: C, 58.13; H, 3.83; N, 4.84%.

4.1.4. 2-Formyl-5-methoxy-3-(4-nitrophenoxy) phenylacetate (***8***)

A solution of 2-hydroxy-4-methoxy-6-(4-nitrophenoxy) benzaldehyde **7** (0.4 g, 1.4 mmol) and triethylamine (0.4 ml, 2.8 mmol) in dry DCM (10 ml) was stirred under nitrogen at 0 °C and treated drop wise with acetyl chloride (0.1 ml, 1.5 mmol). After 1 h, the solution was allowed to warm to rt and stirred at rt for 6 h, diluted with DCM (20 ml) and washed successively with water (20 ml) and brine (20 ml). The organic layer was separated, dried ($MgSO_4$) and evaporated to dryness. The crude product was chromatographed (petrol/EtOAc, 85:15) to yield the title compound **8** (365 mg, 1.1 mmol, 80% yield) as yellow plates. Mp 136–137 °C. R_f 0.23 (petrol/EtOAc, 7:3). ^1H NMR (300 MHz, $CDCl_3$): δ 10.15 (s, 1H, Ar–CHO), 8.27 (dd, 2H, J_{HH} 7.0, 2.1, Ar–H), 7.14 (dd, 2H, J_{HH} 7.0, 2.1, Ar–H), 6.53 (d, 1H, J_{HH} 2.3, Ar–H), 6.39 (d, 1H, J_{HH} 2.3, Ar–H), 3.85 (s, 3H, OMe), 2.40 (s, 3H, OCOMe). ^{13}C NMR (75 MHz, $CDCl_3$): 185.30 (Ar–CHO), 169.15 (CO), 165.53, 161.80, 159.99, 153.10, 143.77, 126.24, 118.25, 114.08, 106.45, 103.92, 56.14 (OMe), 20.97 (OCOMe). ν_{max}/cm^{-1}: 3346, 3118, 3073, 2893, 1755 (CO), 1679 (CO), 1615, 1485, 1437, 1367; m/z (ES): 332 (M^++1); Found: C, 57.8; H, 4.0; N, 4.3%. $C_{16}H_{13}NO_7$ requires: C, 58.01; H, 3.96; N, 4.23%.

4.1.5. (S)-2-((1-Amino-3-(4-hydroxyphenyl)-1-oxopropan-2-ylamino)methyl)-5-methoxy-3-(4-nitrophenoxy) phenylacetate (***9***)

$NaBH(OAc)_3$ (200 mg, 0.9 mmol) was added to a stirred solution of 2-formyl-5-methoxy-3-(4-nitrophenoxy)phenylacetate **8** (100 mg, 0.3 mmol) with L-tyrosinamide (54 mg, 0.3 mmol) and acetic acid (5 ml) in DCM/THF (20 ml) and the resulting mixture was stirred at rt for 15 h. The reaction mixture was diluted with EtOAc (50 ml) and washed with water (20 ml) and brine (20 ml). The organic phase was separated, dried ($MgSO_4$) and concentrated by rotary evaporation. Purification using chromatography (DCM/MeOH, 99:1 to 95:5) yielded the title compound **9** (80 mg, 0.16 mmol, 53% yield) as

pale yellow prisms. Mp 129–130 °C. R_f 0.31 (DCM/MeOH, 95:5). $[\alpha]_D$ −136 (*c* 0.10, MeOH). ^{1}H NMR (300 MHz, MeOD): δ 8.11 (dd, 2H, J_{HH} 7.1, 2.0, Ar–H), 6.87 (dd, 2H, J_{HH} 7.1, 2.0, Ar–H), 6.75 (d, 2H, J_{HH} 8.4, Ar–H), 6.46 (d, 2H, J_{HH} 8.4, Ar–H), 6.22 (d, 1H, J_{HH} 2.3, Ar–H), 5.95 (d, 1H, J_{HH} 2.3, Ar–H), 4.22 (d, 1H, J_{HH} 14.5, Ar–CH_2–NH), 3.71 (dd, 1H, J_{HH} 9.9, 5.3, NH–CH–CONH$_2$), 3.57 (s, 3H, OMe), 3.51 (d, 1H, J_{HH} 14.5, Ar–CH_2–NH), 3.15 (dd, 1H, J_{HH} 13.8, 10.0, Ar–CH_2–CH–CONH$_2$), 3.06 (dd, 1H, J_{HH} 13.8, 5.3, Ar–CH_2–CH–CONH$_2$), 2.14 (s, 3H, CO$_2$Me). ^{13}C NMR (75 MHz, MeOD): 176.00 (CONH$_2$), 174.26 (COMe), 164.06, 163.41, 160.34, 157.25, 156.76, 144.69, 131.60, 130.71, 127.34, 118.89, 116.65, 108.29, 100.20, 99.09, 64.24, 56.29 (OMe), 45.82, 34.08, 23.14 (COMe). ν_{max}/cm^{-1}: 3298, 1673 (CO), 1600, 1514, 1398, 1236, 1142, 1110, 1056; *m*/*z* (ES): 496 (M$^+$+1). Calculated accurate mass: 518.1539; $C_{25}H_{25}N_3O_8Na$ requires: 518.1542.

4.1.6. (S)-2-((1-Amino-1-oxo-3-phenylpropan-2-ylamino)methyl)-5-methoxy-3-(4-nitrophenoxy) phenylacetate (**10**)

NaBH(OAc)$_3$ (384 mg, 1.8 mmol) was added to a stirred solution of 2-formyl-5-methoxy-3-(4-nitrophenoxy) phenylacetate **8** (200 mg, 0.6 mmol) with L-phenylalanine amide (100 mg, 0.6 mmol) and acetic acid (2 ml) in DCM/THF (20 ml) and the resulting mixture was stirred at rt for 15 h. The reaction mixture was diluted with EtOAc (50 ml) and washed with water (20 ml) and brine (20 ml). The organic phase was separated, dried ($MgSO_4$) and concentrated by rotary evaporation. Purification using chromatography (DCM/MeOH, 99:1 to 95:5) yielded the title compound **10** (90 mg, 0.19 mmol, 31% yield) as colourless plates. Mp 193–195 °C. R_f 0.37 (DCM/MeOH, 9:1). $[\alpha]_D$ −72 (*c* 0.10, MeOH). ^{1}H NMR (300 MHz, MeOD): δ 8.15 (dd, 2H, J_{HH} 7.0 and 2.1, Ar–H), 7.03 (m, 5H, Ar–H), 6.92 (dd, 2H, J_{HH} 7.0 and 2.1, Ar–H), 6.22 (d, 1H, J_{HH} 2.3, Ar–H), 5.96 (d, 1H, J_{HH} 2.3, Ar–H), 4.22 (d, 1H, J_{HH} 14.5, Ar–CH_2–NH), 3.8 (dd, 1H, J_{HH} 9.9 and 5.3, NH–CH–CONH$_2$), 3.59 (s, 3H, OMe), 3.47 (d, 1H, J_{HH} 14.5, Ar–CH_2–NH), 3.24 (d, 2H, J_{HH} 4.1 Hz, Ar–CH_2–CH–CONH$_2$), 2.15 (s, 3H, CO$_2$Me). ^{13}C NMR (75 MHz, MeOD): 175.75 (CONH$_2$), 174.26 (COMe), 164.03, 163.46, 160.35, 156.80, 140.19, 130.64, 129.71, 127.76, 127.32, 118.97, 108.20, 100.14, 98.95, 63.95, 56.23 (OMe), 45.67, 35.01, 30.97, 23.14 (COMe). ν_{max}/cm^{-1}: 3431, 3086, 2940, 1673 (CO), 1622, 1514, 1434, 1343, 1236, 1143; *m*/*z* (ES): 502 (M+Na$^+$). Calculated accurate mass: 502.1590; $C_{25}H_{25}N_3O_7Na$ requires: 502.1577.

4.1.7. (S)-2-((1-Amino-3-(4-hydroxyphenyl)-1-oxopropan-2-ylamino)methyl)-3-(4-aminophenoxy)-5-methoxy phenylacetate (**11**)

A slurry of PtO_2 (1.1 mg, 4.0 mol % of 81% catalyst) was stirred in EtOAc (5 ml) while bubbling nitrogen through the mixture. A solution of (*S*)-2-((1-amino-3-(4-hydroxyphenyl)-1-oxopropan-2-ylamino)methyl)-5-methoxy-3-(4-nitrophenoxy) phenylacetate **9** (60 mg, 0.12 mmol) in EtOAc (10 ml) was added and the purging continued. Hydrogen gas was then purged into the flask and the resulting mixture was stirred at rt for 15 h. After completion of reaction (TLC), reaction mixture was filtered through a pad of Celite and taken to dryness by rotary evaporation. The crude product was chromatographed (DCM/MeOH, 95:5) to yield the title compound **11** (28 mg, 0.06 mmol, 50% yield) as off white prisms. Mp 132–133 °C. R_f 0.25 (DCM/MeOH, 95:5). $[\alpha]_D$ −120 (*c* 0.10, MeOH). ^{1}H NMR (300 MHz, MeOD): δ 6.92 (d, 2H, J_{HH} 8.3, Ar–H), 6.79 (s, 4H, Ar–H), 6.61 (d, 2H, J_{HH} 8.3, Ar–H), 6.13 (d, 1H, J_{HH} 2.0, Ar–H), 5.76 (d, 1H, J_{HH} 2.0, Ar–H), 4.41 (d, 1H, J_{HH} 14.3, Ar–CH_2–NH), 4.01 (dd, 1H, J_{HH} 9.9 and 5.3, NH–CH–CONH$_2$), 3.89 (d, 1H, J_{HH} 14.3, Ar–CH_2–NH), 3.62 (s, 3H, OMe), 3.15 (dd, 1H, J_{HH} 13.8 and 10.0, Ar–CH_2–CH–CONH$_2$), 3.06 (dd, 1H, J_{HH} 13.8 and 5.3, Ar–CH_2–CH–CONH$_2$), 2.28 (s, 3H, CO$_2$Me). ^{13}C NMR (75 MHz, MeOD): 176.33 (CONH$_2$), 174.06 (COMe), 162.97, 161.01, 159.75, 157.23, 148.94, 145.89, 131.78, 130.71, 122.26, 118.06, 116.33, 105.43, 96.66, 95.47, 3.69, 55.90 (OMe), 45.37, 34.16, 22.96 (COMe). ν_{max}/cm^{-1}: 3351, 1673 (CO), 1586, 1501, 1206, 1142, 1057, 825; *m*/*z* (ES): 466 (M$^+$+1). Calculated accurate mass: 488.1798; $C_{25}H_{27}N_3O_6Na$ requires: 488.1783.

4.1.8. (S)-2-((1-Amino-1-oxo-3-phenylpropan-2-ylamino)methyl)-3-(4-amino phenoxy)-5-methoxy phenylacetate (**12**)

A slurry of PtO_2 (0.95 mg, 4.0 mol % of catalyst) was stirred in EtOAc (5 ml) while bubbling nitrogen through the mixture. A solution of (*S*)-2-((1-amino-1-oxo-3-phenylpropan-2-ylamino) methyl)-5-methoxy-3-(4-nitrophenoxy) phenylacetate **10** (50 mg, 0.1 mmol) in EtOAc (10 ml) was added and the purging continued. Hydrogen gas was then purged into the flask and the resulting mixture was stirred at rt for 15 h. After completion of reaction (TLC), reaction mixture was filtered through a pad of Celite and taken to dryness by rotary evaporation. The crude product was chromatographed (DCM/MeOH, 9:1) to yield the title compound **12** (25 mg, 0.06 mmol, 54% yield) as colourless needles. Mp 106–108 °C. R_f 0.47 (DCM/MeOH, 9:1). $[\alpha]_D$ −116 (*c* 0.10, MeOH). ^{1}H NMR (300 MHz, MeOD): δ 7.05 (dd, 2H, J_{HH} 5.0, 1.6, Ar–H), 7.00 (m, 3H, Ar–H), 6.67 (m, 4H, Ar–H), 6.01 (d, 1H, J_{HH} 2.3 Hz, Ar–H), 5.63 (d, 1H, J_{HH} 2.3 Hz, Ar–H), 4.27 (d, 1H, J_{HH} 14.3 Hz, NH–CH–CONH$_2$), 3.95 (t, 1H, J_{HH} 7.5 Hz, Ar–CH_2–CH-CONH$_2$), 3.69 (d, J_{HH} 14.3 Hz, Ar–CH_2–CH-CONH$_2$), 3.50 (s, 3H, OMe), 3.26 (d, 2H, J_{HH} 7.3 Hz, Ar–CH_2–NH), 2.17 (s, 3H, Me). ^{13}C NMR (75 MHz, MeOD): 176.12 (CONH$_2$), 174.09 (COMe), 162.99, 160.99, 159.75, 148.85, 145.96, 140.19, 130.86, 129.71, 127.69, 122.27, 118.03, 105.30, 96.66, 95.45, 63.47, 55.91 (OMe), 45.30, 35.11, 22.96 (COMe). ν_{max}/cm^{-1}: 3353, 1673 (CO), 1594, 1503, 1429, 1364, 1207, 1143, 1058; *m*/*z* (ES): 472 (M+Na$^+$). Calculated accurate mass: 472.1848; $C_{25}H_{27}N_3O_5Na$ requires: 472.1840.

Acknowledgements

The authors gratefully acknowledge the financial support provided by the Dorothy Hodgkin Postgraduate Award from Research Council UK (to A.K.A.), and I. Chopra, A. O'Neill, K. Miller, J. Hurdle and A. Al-Omar for help and advice.

References and notes

1. Binder, S.; Levitt, A. M.; Sacks, J. J.; Hughes, J. M. *Science* **1999**, *284*, 1311–1313.
2. Schmidt, F. R. *Appl. Microbiol. Biotechnol.* **2004**, *63*, 335–343.
3. Moellering, R. C. *Clin. Infect. Dis.* **1998**, *27*, S135–S140.
4. Chopra, I. *Curr. Opin. Microbiol.* **1998**, *1*, 495–501.
5. Record, M. T. J. *Cellular and Molecular Biology*; ASM: Washington, DC, 1996, pp 792–820.
6. Villain-Guillot, P.; Bastide, L.; Gualtieri, M.; Leonetti, J.-P. *Drug Discovery Today* **2007**, *12*, 200–208.
7. Campbell, E. A.; Korzheva, N.; Mustaev, A.; Murakami, K.; Nair, S.; Goldfarb, A.; Darst, S. A. *Cell* **2001**, *104*, 901–912.
8. Mitchison, D. A. *Int. J. Tuber. Lung Dis.* **2000**, *4*, 796–806.
9. Sensi, P. *Rev. Infect. Dis.* **1983**, *5*, S402–S406.
10. Schrenzel, J.; Harbarth, S.; Schockmel, R.; Genne, D.; Bregenzer, T.; Flueckiger, U.; Petignat, C.; Jacobs, F.; Francioli, P.; Zimmerli, W.; Lew, D. P. *Clin. Infect. Dis.* **2004**, *39*, 1285–1292.
11. Barluenga, J.; Aznar, F.; Garcia, A. B.; Cabal, M. P.; Palacios, J. J.; Menendez, M. A. *Bioorg. Med. Chem. Lett.* **2006**, *16*, 5717–5722.
12. Murphy, C. K.; Mullin, S.; Osburne, M. S.; van Duzer, J.; Siedlecki, J.; Yu, X.; Kerstein, K.; Cynamon, M.; Rothstein, D. M. *Antimicrob. Agents Chemother.* **2006**, *50*, 827–834.
13. Rothstein, D. M.; Farquhar, R. S.; Sirokman, K.; Sondergaard, K. L.; Hazlett, C.; Doye, A. A.; Gwathmey, J. K.; Mullin, S.; van Duzer, J.; Murphy, C. K. *Antimicrob. Agents Chemother.* **2006**, *50*, 3658–3664.
14. Rothstein, D. M.; Shalish, C.; Murphy, C. K.; Sternlicht, A.; Campbell, L. A. *Expert Opin. Investig. Drugs* **2006**, *15*, 603–623.
15. Zorov, S. D.; Yuzenkova, J. V.; Severinov, K. V. *Mol. Biol.* **2006**, *40*, 875–884.
16. Payne, D. J.; Gwynn, M. N.; Holmes, D. J.; Pompliano, D. L. *Nat. Rev. Drug Discovery* **2007**, *6*, 29–40.
17. Besong, G. E.; Bostock, J. M.; Stubbings, W.; Chopra, I.; Roper, D. I.; Lloyd, A. J.; Fishwick, C. W. G.; Johnson, A. P. *Angew. Chem., Int. Ed.* **2005**, *44*, 6403–6406.
18. Horton, J. R.; Bostock, J. M.; Chopra, I.; Hesse, L.; Phillips, S. E. V.; Adams, D. J.; Johnson, A. P.; Fishwick, C. W. G. *Bioorg. Med. Chem. Lett.* **2003**, *13*, 1557–1560.

19. Heikkila, T.; Ramsey, C.; Davies, M.; Galtier, C.; Stead, A. M. W.; Johnson, A. P.; Fishwick, C. W. G.; Boa, A. N.; McConkey, G. A. *J. Med. Chem.* **2007**, *50*, 186–191.
20. Heikkila, T.; Thirumalairajan, S.; Davies, M.; Parsons, M. R.; McConkey, A. G.; Fishwick, C. W. G.; Johnson, A. P. *Bioorg. Med. Chem. Lett.* **2006**, *16*, 88–92.
21. Grzybowski, B. A.; Ishchenko, A. V.; Kim, C. Y.; Topalov, G.; Chapman, R.; Christianson, D. W.; Whitesides, G. M.; Shakhnovich, E. I. *Proc. Natl. Acad. Sci. U.S.A.* **2002**, *99*, 1270–1273.
22. Han, Q.; Dominguez, C.; Stouten, P. F. W.; Park, J. M.; Duffy, D. E.; Galemmo, R. A.; Rossi, K. A.; Alexander, R. S.; Smallwood, A. M.; Wong, P. C.; Wright, M. M.; Luettgen, J. M.; Knabb, R. M.; Wexler, R. R. *J. Med. Chem.* **2000**, *43*, 4398–4415.
23. Honma, T.; Hayashi, K.; Aoyama, T.; Hashimoto, N.; Machida, T.; Fukasawa, K.; Iwama, T.; Ikeura, C.; Ikuta, M.; Suzuki-Takahashi, I.; Iwasawa, Y.; Hayama, T.; Nishimura, S.; Morishima, H. *J. Med. Chem.* **2001**, *44*, 4615–4627.
24. Schneider, G.; Clement-Chomienne, O.; Hilfiger, L.; Schneider, P.; Kirsch, S.; Bohm, H. J.; Neidhart, W. *Angew. Chem., Int. Ed.* **2000**, *39*, 4130–4133.
25. Gillet, V.; Johnson, A. P.; Mata, P.; Sike, S.; Williams, P. *J. Comput. Aided Mol. Des.* **1993**, *7*, 127–153.
26. Gillet, V. J.; Myatt, G.; Zsoldos, Z.; Johnson, A. P. *Perspect. Drug Discovery Des.* **1995**, *3*, 34–50.
27. Gillet, V. J.; Newell, W.; Mata, P.; Myatt, G.; Sike, S.; Zsoldos, Z.; Johnson, A. P. *J. Chem. Inf. Comput. Sci.* **1994**, *34*, 207–217.
28. Broadhurst, M. J.; Hassall, C. H.; Thomas, G. J. *J. Chem. Soc., Perkin Trans. 1* **1977**, 2502–2512.
29. Ohmichi, T.; Maki, A.; Kool, E. T. *Proc. Natl. Acad. Sci. U.S.A.* **2002**, *99*, 54–59.
30. Paulini, R.; Lerner, C.; Diederich, F.; Jakob-Roetne, R.; Zurcher, G.; Borroni, E. *Helv. Chim. Acta* **2006**, *89*, 1856–1887.
31. Paulini, R.; Lerner, C.; Jakob-Roetne, R.; Zurcher, G.; Borroni, E.; Diederich, F. *Chembiochem* **2004**, *5*, 1270–1274.